Article

AMERICAN ORTHOPAEDIC FOOT & ANKLE SOCIETY

Foot & Ankle International®
2025, Vol. 46(1) 71–82

DOI: 10.1177/10711007241298672
journals.sagepub.com/home/fai

Comparative Analysis of Structural Differences in Progressive Collapsing Foot Deformity With and Without Hallux Valgus

Chien-Shun Wang, MD[1,2], Erik Jesús Huánuco Casas, MD[3,4], Grayson M. Talaski[5], Antoine S. Acker, MD[3,6], Mark E. Easley, MD[3], and Cesar de Cesar Netto, MD, PhD[3]

Abstract

Background: Progressive collapsing foot deformity (PCFD) and hallux valgus (HV) are complex 3-dimensional deformities of the foot. This study aimed to investigate structural and alignment differences between PCFD with and without HV using weightbearing computed tomography.

Methods: Patients with PCFD aged 18 years or older who underwent weightbearing computed tomography were consecutively enrolled. Standard 2-dimensional PCFD and HV parameters were assessed semiautomatically. Foot and ankle offset, forefoot arch angle, and pronation of the medial column bones in the coronal plane, with the ground as a reference, were manually measured. Additionally, the angles from the inferior aspect of subtalar posterior facet of the talus to the ground (subtalar horizontal angle), from the inferior (posterior facet) to superior facets of the talus (infratalar-supratalar angle), and from the inferior (posterior facet) of the talus to the superior facet of the calcaneus (infratalar-supracalcaneal angle) were examined. HV deformity was defined by an HV angle of ≥15 degrees.

Results: Among 72 feet (58 patients) studied, 33 displayed HV, whereas 39 did not. In the coronal plane, the PCFD with HV group showed a higher infratalar-supratalar angle and greater pronation at the first tarsometatarsal joint, first metatarsal bone, and head. The PCFD with HV group also exhibited greater naviculocuneiform joint supination. Generalized estimating equation logistic regression analysis revealed significant associations of HV deformity with the intrinsic rotation of the first metatarsal bone ($P < .001$), infratalar-supratalar angle ($P = .004$), and rotation of the first tarsometatarsal joint ($P < .001$).

Conclusion: This study confirmed significant structural and alignment differences between PCFD with and without HV. Notably, the infratalar-supratalar angle, rotation of the first tarsometatarsal joint, and intrinsic rotation of the first metatarsal bone were associated with HV deformity.

Level of Evidence: Level III, retrospective comparative study.

Keywords: progressive collapsing foot deformity, hallux valgus, weightbearing computed tomography, overpronated deformity

[1]Division of Orthopaedic Trauma, Department of Orthopaedics and Traumatology, Taipei Veterans General Hospital, Taipei, Taiwan
[2]Department of Orthopaedics, School of Medicine, National Yang Ming Chiao Tung University, Taipei, Taiwan
[3]Division of Foot and Ankle Surgery, Department of Orthopaedic Surgery, Duke University School of Medicine, Durham, NC, USA
[4]Department of Traumatology and Orthopedics, Delgado Clinic, Lima-Perú
[5]Department of Orthopedics and Rehabilitation, University of Iowa, Iowa City, IA, USA
[6]Centre of Foot and Ankle Surgery, Clinique La Colline, Geneva, Switzerland

Corresponding Author:
Cesar de Cesar Netto, MD, PhD, Division of Foot and Ankle Surgery, Department of Orthopaedic Surgery, Duke University School of Medicine, 2927 40 Duke Medicine Circle 124 Davison Building, Durham, NC 27710, USA.
Email: cesar.netto@duke.edu

Introduction

Progressive collapsing foot deformity (PCFD) and hallux valgus (HV) are common foot deformities. Concurrently, these 2 conditions share certain morphologic similarities. Classic PCFD includes hindfoot and midfoot hyperpronation in the coronal plane.[10,15,19] Similarly, HV deformity is purported to be associated with first metatarsal overpronation deformity.[22,26,32,39,41] Nonetheless, the relationship between these 2 deformities has not yet been extensively discussed.

The relationship between hindfoot and forefoot deformities has become increasingly evident with the introduction of weightbearing computed tomography (WBCT). Bakshi et al[4] identified a significant association between hindfoot valgus and first metatarsal pronation. Steadman et al[38] reported that this correlation was notably more pronounced in patients with an abnormal Meary angle. However, first metatarsal pronation has been recognized as a component of HV deformity[7,11,22,28,31,39] and may contribute to poor outcomes and recurrence following operative interventions for this pathology.[5,21,22,35] The relationship between the HV angle and pes planus remains unclear in plain-film radiography studies[3,8,40] and large-scale studies on disease prevalence.[6,33]

PCFD constitutes a spectrum of deformities that affect various segments of the foot in divergent magnitudes.[1,17,27] The present study aimed to investigate structural and alignment differences between PCFD with and without HV using WBCT. We hypothesized that there are distinct hindfoot or midfoot structural or alignment variances between PCFD with and without HV deformity.

Materials and Methods

This retrospective analysis was approved by the Institutional Review Board of the enrolling institution and was conducted in accordance with the principles embodied in the Declaration of Helsinki. The requirement for the acquisition of informed consent from patients was waived owing to the retrospective nature of this study.

This study included patients aged ≥18 years who were clinically diagnosed with PCFD by one of our senior authors and underwent WBCT as part of the standard-of-care evaluation. Patients were consecutively enrolled from May 2023 to December 2023. The diagnostic criteria for PCFD included planovalgus foot deformity combined with medial midfoot pain, with or without lateral hindfoot pain. Patients who had an operative history of ipsilateral foot and ankle fusion/osteotomy or who underwent any HV correction surgery were excluded. Demographic data, including age, sex, body mass index (BMI), and rigid deformity, were collected through chart review.

Radiographic Evaluation

WBCT was performed using a cone-beam CT extremity scanner (pedCAT or HiRise model; CurveBeam, Warrington, PA, USA). The collected data sets were screened and transformed into DICOM files using the built-in software (CubeVue; CurveBeam). Parameters such as the talar–first metatarsal angle (axial and sagittal), calcaneal inclination angle,[37] hindfoot moment arm,[36] hindfoot angle, axial talonavicular angle, sagittal first tarsal–metatarsal angle, first tarsal–metatarsal angle joint minimum gap, intermetatarsal (IM) angle, and HV angle were semiautomatically measured using Bonelogic foot and ankle software version 2.1.4 (DISIOR, Helsinki, Finland), as previously described.[23,42] The sagittal first tarsal–metatarsal angle was defined as the angle formed between the longitudinal axes of the first metatarsal bone and the medial cuneiform in the sagittal plane.[14] The first tarsal–metatarsal joint minimum gap was defined as the shortest distance measured from the medial cuneiform joint surface to the first metatarsal bone.[29] HV was deemed to be present if the HV angle was ≥15 degrees[20] (Figure 1).

Two fellowship-trained foot and ankle surgeons independently, randomly, and masked performed manual measurements using CubeVue software. Pronation and supination were quantified using positive and negative rotation values, respectively. The measurement protocol and sequence were as follows.

1. Foot and ankle offset[30] was automatically calculated using the Torque Ankle Lever Arm System (TALAS) system after annotating the weightbearing points of the first and fifth metatarsal heads, calcaneus, and the most central and highest point of the talus.
2. The axial plane was aligned parallel to the long axis of the talus, defined as the line from the midpoint of the talar body to its head. The coronal plane was synchronized with the sagittal view at the midpoint of the anteroposterior dimension of the posterior facet to assess talar posterior facet parameters. The subtalar horizontal angle[34] (the angle between the inferior facet and horizontal), infratalar-supratalar angle[34] (the angle between the inferior and superior facets), and infratalar-supracalcaneal angle[34] (the angle between the inferior facet of the talus and superior facet of the calcaneus) were all measured.
3. The axial plane axis was realigned parallel to the long axis of the second metatarsal to measure the forefoot arch angle[18] (the angle between the horizontal and the line drawn from the inferior aspect of the medial cuneiform to the inferior aspect of the fifth metatarsal). Additionally, the rotational profile along the medial column[16] was assessed, including the navicular (the angle between the horizontal and the widest mediolateral distance of the navicular at a level just distal to the most distal aspect of the talonavicular joint), medial cuneiform (the angle between the vertical line and a bisecting line of an

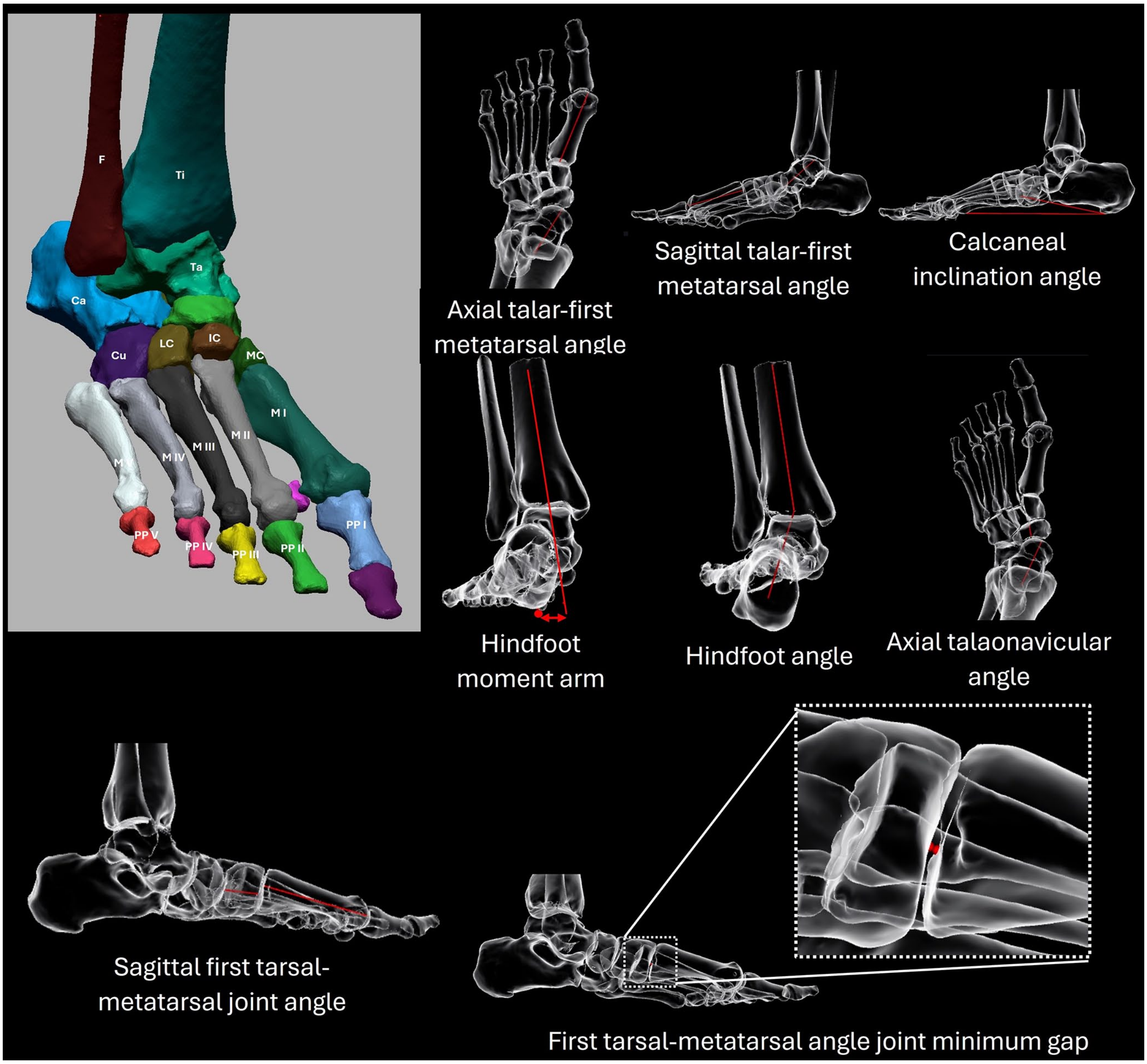

Figure 1. The process of obtaining semiautomated measured parameters using the Bonelogic Foot and Ankle software. Following the upload of DICOM files and manual annotation of the foot bones (top left), the software automatically calculates the relevant parameters based on these annotations.

angle formed by tangent lines to the medial and lateral surfaces of the medial cuneiform at a level just proximal to the most proximal aspect of the first tarsometatarsal joint), first metatarsal base (the angle between the vertical line and a bisecting line of an angle formed by tangent lines to the medial and lateral surfaces of the first metatarsal bone at a level just distal to the most distal aspect of the first tarsometatarsal joint), and first metatarsal head using the α angle[22] (the angle between the vertical line and the line connecting the midpoint of medial and lateral dorsal corners and the midpoint of lateral and medial edges of the sulcus of the first metatarsal head). The rotation of the naviculocuneiform joint was determined by calculating the difference between the navicular rotation angle and medial cuneiform angle. Similarly, the rotation of the first tarsometatarsal joint was determined by subtracting the medial cuneiform angle from the first metatarsal base angle. The intrinsic rotation of the first metatarsal bone was determined by subtracting the first metatarsal base angle from the α angle (Figure 2).

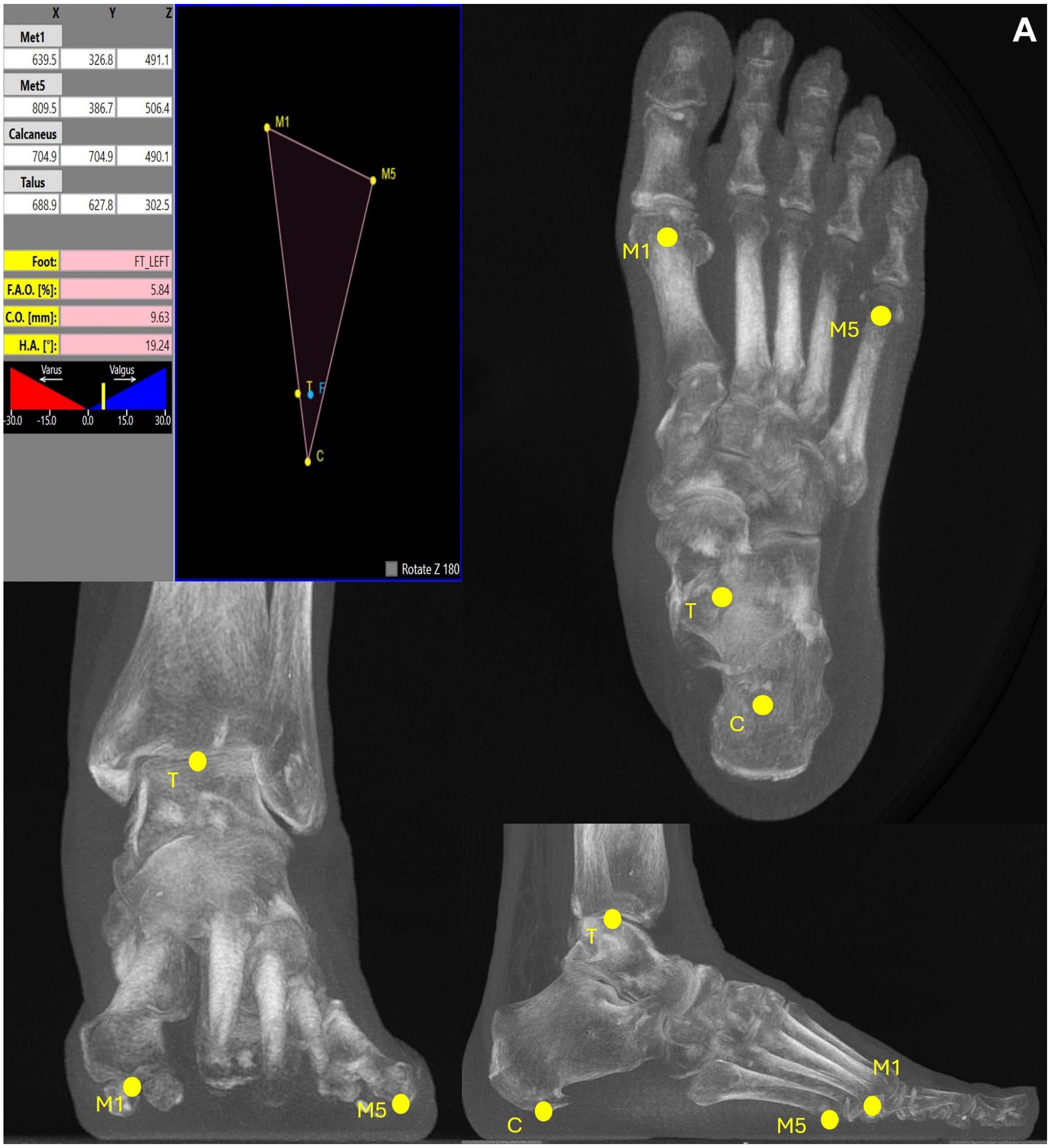

Figure 2. (continued)

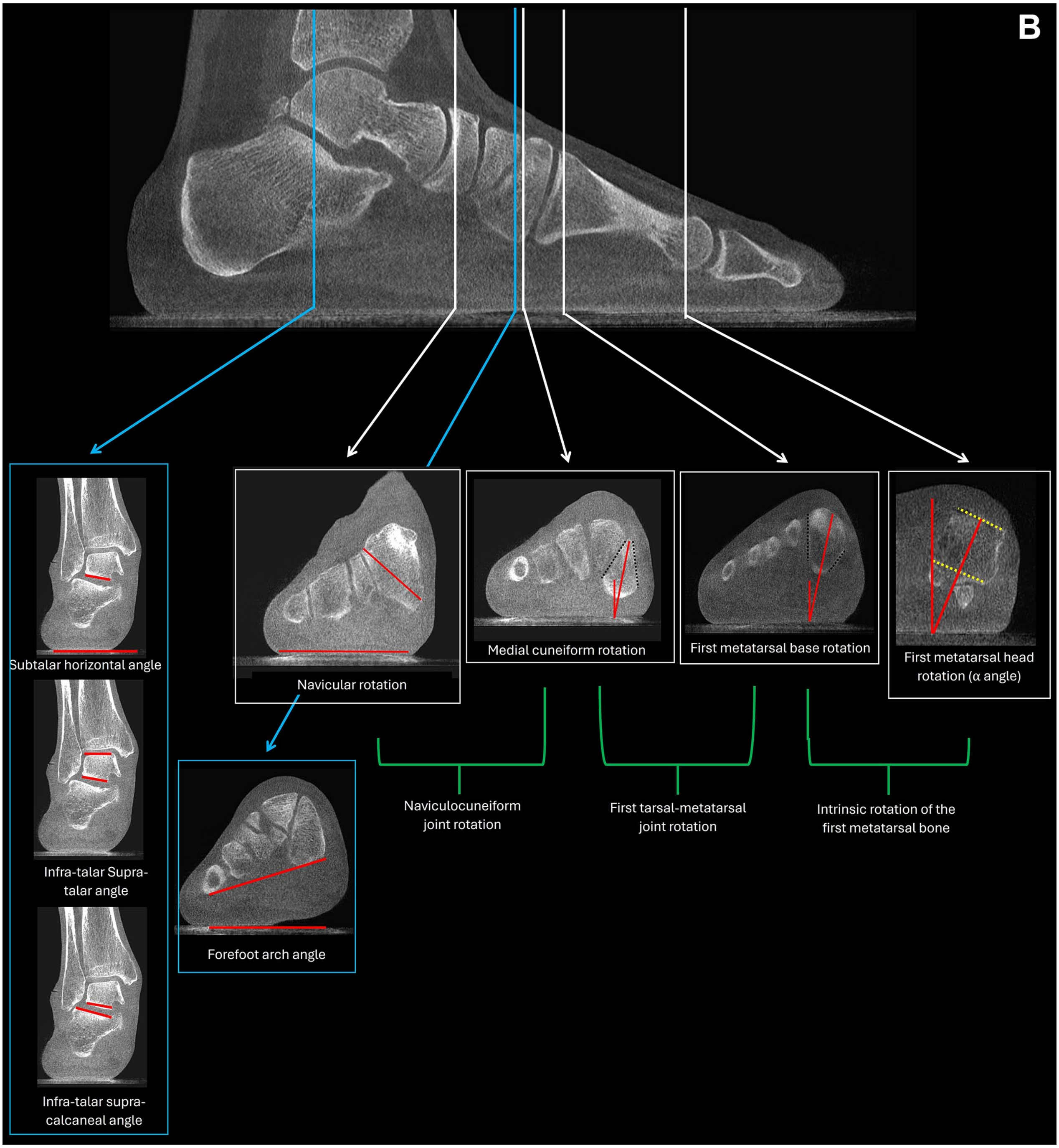

Figure 2. Depiction of radiographic parameters of manually measured radiographic parameters. (A) The CubeVue software screen view with the Torque Ankle Lever Arm System (TALAS) (top left) was used. Three-dimensional coordinates (*x*, *y*, *z* planes) were recorded from specific anatomical landmarks for the program to calculate the Foot and Ankle Offset (F.A.O.), the weightbearing point of the first metatarsal head (Met1 or M1), the weightbearing point of the fifth metatarsal head (Met5 or M5), the calcaneal weightbearing point (C), and the central and highest point of the talus (T). The point labeled F represents the optimal position for the ankle joint's center of rotation, located along the bisecting line of the tripod. (B) Solid lines indicate the level of the measurements. Blue lines denote progressive collapsing foot deformity weightbearing computed tomography parameters, and white lines signify medial column rotational profiles. Black dashed lines represent tangent lines of the bone surface. Red lines signify the measurement of each parameter, whereas the green lines illustrate the discrepancy between the 2 sets of measured values. [See online article for color figure.]

Table 1. Interobserver Reliability of Manual Measurements.

Manual Measurements	Intraclass Correlation Coefficient (95% CI)
Foot and ankle offset	0.954 (0.927–0.971)
Subtalar horizontal angle	0.924 (0.878–0.953)
Infratalar-supratalar angle	0.958 (0.934–0.974)
Infratalar-supracalcaneal angle	0.811 (0.715–878)
Forefoot arch angle	0.979 (0.967–0.987)
Navicular rotation	0.965 (0.945–0.978)
Medial cuneiform rotation	0.963 (0.942–0.977)
First metatarsal base	0.880 (0.814–0.923)
First metatarsal head (α angle)	0.929 (0.869–0.960)

Statistical Analyses

Statistical analyses were performed using R software (version 4.3.1; The R Foundation, Vienna, Austria). Interobserver reliability was examined using intraclass correlation coefficients (ICCs). The normality of variable distribution was assessed using the Shapiro-Wilk test and a distribution histogram. The generalized estimating equation (GEE) method was employed for parameter selection between groups to address the issue of nonindependence between data from bilateral cases. Adjusted P values were obtained using the Benjamini-Hochberg method. Effect sizes were calculated using odds ratios.[9] To avoid being limited by an HV angle ≥15 degrees as the definition of HV deformity, we analyzed the correlation of each parameter with the absolute HV angle and IM angle in our study. The relationships between normally distributed parameters were analyzed using Pearson correlation coefficients, whereas Spearman correlation coefficients were used for non-normally distributed variables. Point-biserial correlations were used for the categorical variables. Parameters with an adjusted P value <.1, an effect size >0.8, or those showing a significant correlation with the HV angle were selected for the GEE logistic regression analysis.

Results

A total of 58 patients (median age: 62 [20.5] years), corresponding to 72 feet, were included in this study. Within this cohort, 39 patients (67.2%) were female, and the median BMI was 32.6 (9.0) kg/m^2. In 33 (45.8%) cases, the left foot was involved. Manual measurements exhibited excellent interobserver reliability, with ICCs ranging from 0.811 to 0.979 (Table 1). The patient cohort analyzed in this study presented with an average foot and ankle offset of 8.4% ± 3.7%, a sagittal talar–first metatarsal angle of −27.8 ± 11.2 degrees, a calcaneal inclination angle of 12.7 ± 5.31 degrees, and a median axial talonavicular angle of 47.6 (12.9) degrees.

On the basis of our definition of HV deformity, 39 feet were included in the PCFD without HV group, whereas 33 feet were assigned to the PCFD with HV group. The mean HV angle in the PCFD without HV group was 6.4 ± 6.1 degrees, with an IM angle of 10.8 ± 3.3 degrees. In the PCFD with HV group, 9 of 33 feet (27.27%) exhibited symptoms related to hallux valgus, with a mean HV angle of 23.8 ± 6.7 degrees and an IM angle of 14.8 ± 3.2 degrees. The results of the GEE parameter selection between groups are presented in Table 2. Demographic data, including age, sex, BMI, left side, and percentage of rigid deformity, were similar between the groups. However, the effect size was high (0.892) for female participants. Among the radiographic parameters, significant valgus of the infratalar-supratalar angle (P=.022), pronation at the first tarsometatarsal joint (P=.064), intrinsic pronation of the first metatarsal bone (P=.064), pronation at the first metatarsal head (α angle) (P=.022), and supination at the naviculocuneiform joint (P=.035) were observed in the PCFD with HV group and were selected for further regression analysis.

Table 3 presents the correlation coefficients for HV deformity. The axial tarsal-first metatarsal angle (ρ=−0.311, P=.008), rotation of the first metatarsal head (α angle) (ρ=0.312, P=.008), rotation of the first tarsometatarsal joint (r=0.348, P=.003), and infratalar-supratalar angle (ρ=0.389, P=.001) were weakly correlated with the HV angle. The rotation of the naviculocuneiform joint was moderately correlated with the HV angle (ρ=−0.506, P<.001). Regarding the IM angle, the infratalar-supratalar angle (ρ=0.263, P=.026), rotation of the first tarsometatarsal joint (r=0.290, P=.013), and axial tarsal-first metatarsal angle (ρ=−0.415, P<.001) showed a weak correlation, whereas rotation of the naviculocuneiform joint exhibited a moderate correlation (ρ=−0.519, P<.001).

Female sex and the radiographic parameters shown in Figure 3 were entered into the GEE logistic regression analysis. Owing to convergence issues with the initial model, a stepwise parameter selection approach was applied, iteratively eliminating parameters with the smallest effect sizes or the largest P values until the model converged. Eliminating parameters with the smallest effect sizes resulted in the best Quasi-likelihood under the Independence model Criterion (QIC) value, and this model was adopted. The results showed that the infratalar-supratalar angle (P=.004), first tarsal–metatarsal joint (P<.001), and intrinsic rotation of the first metatarsal bone (P<.001) were significantly associated with the presence of HV deformity (Table 4). The marginal R-squared value and QIC

Table 2. Generalized Estimating Equation Parameter Selection Between the PCFD Without HV Group and the PCFD With HV Group.

	PCFD without HV (n = 39)	PCFD with HV (n = 33)	Adjusted *P* Value[a]	Effect Size
Demographic parameters				
Age, y, median (IQR)	63 (20)	65 (13)	>.999	.554
Female sex, n (%)	20 (64.5%)	19 (70.4%)	.830	.892[b]
BMI, median (IQR)	31.4 (12.6)	32.9 (7.2)	.830	.564
Left side, n (%)	17 (43.6%)	16 (48.5%)	>.999	.539
Rigid deformity, n (%)	11 (28.2%)	10 (30.3%)	.908	.681
Semiautomated measured parameters				
Axial talar–first metatarsal angle, degrees, median (IQR)	31.7 (15.7)	27.1 (12.7)	.441	.531
Sagittal talar–first metatarsal angle, degrees, mean ± SD	−27.6 ± 11.2	−28.0 ± 11.5	>.999	.552
Calcaneal inclination angle, degrees, mean ± SD	13.3 ± 5.1	12.0 ± 5.6	.830	.536
Hindfoot moment arm, mm, mean ± SD	12.9 ± 7.1	13.5 ± 7.8	.830	.566
Hindfoot angle, degrees, mean ± SD	29.8 ± 6.5	32.0 ± 6.4	.441	.586
Axial talonavicular angle, degrees, median (IQR)	47.0 (11.4)	48.4 (13.3)	.959	.556
Sagittal first tarsal–metatarsal joint angle, degrees, mean ± SD	9.2 ± 3.1	9.9 ± 3.0	.846	.575
First tarsal–metatarsal joint minimum gap, mm, median (IQR)	1.2 (0.2)	1.1 (0.3)	.846	.325
PCFD weightbearing CT parameters				
Foot and ankle offset, %, mean ± SD	8.7 ± 4.0	8.1 ± 3.4	.830	.527
Subtalar horizontal angle, degrees, mean ± SD	11.7 ± 7.4	15.0 ± 7.0	.265	.589
Infratalar-supratalar angle, degrees, median (IQR)	11.9 (11.2)	18.0 (17.5)	.022[c]	.608
Infratalar-supracalcaneal angle, degrees, mean ± SD	−4.9 ± 3.8	−5.0 ± 4.2	.846	.570
Forefoot arch angle, degrees, mean ± SD	−1.8 ± 6.2	−1.5 ± 5.4	>.999	.554
Medial column rotational profiles				
Navicular, degrees, mean ± SD	34.7 ± 9.0	37.3 ± 9.0	.830	.562
Naviculocuneiform joint, degrees, median (IQR)	−29.6 (8.9)	−35.4 (5.8)	.035[c]	.479
Medial cuneiform, degrees, mean ± SD	5.7 ± 8.2	2.7 ± 7.3	.331	.524
First tarsal–metatarsal joint, degrees, mean ± SD	19.9 ± 7.1	24.5 ± 6.8	.064[c]	.604
First metatarsal base, degrees, mean ± SD	25.6 ± 7.0	27.2 ± 6.5	.830	.566
Intrinsic rotation of the first metatarsal bone, degrees, mean ± SD	−9.1 ± 6.2	−4.1 ± 6.8	.064[c]	.616
First metatarsal head (α angle), degrees, median (IQR)	17.3 (9.3)	21.5 (6.9)	.022[c]	.649

Abbreviations: BMI, body mass index; GEE, generalized estimating equation; HV, hallux valgus; IQR, interquartile range; PCFD, progressive collapsing foot deformity.
[a]Adjusted using the Benjamini-Hochberg method.
[b]Effect size > 0.8.
[c]$P < .1$.

value for this regression model were 0.606 and 45.519, respectively.

Discussion

The present study revealed significant differences between PCFD with and without HV deformity with respect to several parameters. Greater valgus of the infratalar-supratalar angle ($P = .022$), pronated first tarsometatarsal joint ($P = .064$), intrinsic pronation of the first metatarsal bone ($P = .064$), and pronated first metatarsal head (α angle) ($P < .022$) and supinated naviculocuneiform joint ($P = .035$) were identified in the PCFD with HV group. These results were consistent with our hypothesis. Furthermore, the infratalar-supratalar angle, rotation of the naviculocuneiform joint, rotation of the first tarsometatarsal joint, intrinsic rotation of the first metatarsal bone, and axial tarsal–first metatarsal angle were significantly correlated with the absolute values of both the IM and HV angles, whereas the rotation of the first metatarsal head was exclusively correlated with the HV angle. GEE logistic regression analysis indicated that the infratalar-supratalar angle ($P = .004$), rotation of the first tarsometatarsal joint ($P < .001$), and intrinsic rotation of the first metatarsal bone ($P < .001$) were significantly associated with HV deformity.

The differences in the medial column coronal rotation between the PCFD with HV group and the PCFD without HV group aligned with the results of the WBCT analysis conducted by Lalevee et al,[25] who compared medial column

Table 3. Correlation Coefficients for Parameters Relative to the Hallux Valgus Angle and Intermetatarsal Angle.

	Hallux Valgus Angle		Intermetatarsal Angle	
	Correlation Coefficient	*P* Value	Correlation Coefficient	*P* Value
Demographic parameters				
Age	$\rho = -0.46$	.701	$\rho = 0.029$	.807
Female	$r = 0.072$	.547	$r = -0.031$	.793
BMI	$\rho = 0.027$	.823	$\rho = -0.011$	.929
Left side	$r = 0.034$	.775	$r = -0.018$	.883
Rigid deformity	$r = 0.015$	.901	$r = -0.012$	.918
Semiautomated measured parameters				
Axial talar–first metatarsal angle	$\rho = -0.311$	.008**	$\rho = -0.415$	<.001**
Sagittal talar–first metatarsal angle	$r = 0.010$	.931	$r = 0.044$	.713
Calcaneal inclination angle	$r = -0.051$	.670	$r = 0.062$	.604
Hindfoot moment arm	$r = -0.027$	.822	$r = -0.125$	.295
Hindfoot angle	$r = 0.052$	.662	$r = -0.035$	.771
Axial talonavicular angle	$\rho = 0.165$	.166	$\rho = 0.095$	.425
Sagittal first tarsal–metatarsal joint angle	$r = 0.184$	.122	$r = 0.161$	.178
First tarsal–metatarsal joint minimum gap	$\rho = 0.120$	.313	$\rho = 0.216$	.068
PCFD weightbearing CT parameters				
FAO	$r = -0.090$	.451	$r = -0.006$	.963
Subtalar horizontal angle	$r = 0.180$	.131	$r = 0.216$	.068
Infratalar-supratalar angle	$\rho = 0.389$	.001**	$\rho = 0.263$	.026*
Infratalar-supracalcaneal angle	$r = -0.114$	.342	$r = -0.100$	.402
Forefoot arch angle	$r = -0.038$	.750	$r = -0.128$	.282
Medial column rotational profiles				
Navicular	$r = 0.225$	.057	$r = 0.194$	.102
Naviculocuneiform joint	$\rho = -0.506$	<.001**	$\rho = -0.519$	<.001**
Medial cuneiform	$r = -0.177$	.138	$r = -0.188$	.113
First tarsometatarsal joint	$r = 0.348$	.003**	$r = 0.290$	.013*
First metatarsal base	$r = 0.167$	.161	$r = 0.092$	.444
First metatarsal intrinsic torsion	$r = 0.186$	.118	$r = 0.056$	.642
First metatarsal head (α angle)	$\rho = 0.312$	.008**	$\rho = 0.152$	.203

Abbreviations: γ, Pearson correlation coefficient; ρ, Spearman correlation coefficient; BMI, body mass index; CT, Computed Tomography; FAO, Foot and Ankle Offset; PCFD, progressive collapsing foot deformity.
*$P < .05$.
**$P < .01$.

rotation profiles between patients with nonplanovalgus HV (characterized by a normal Meary angle or hindfoot moment arm) and normal controls. Notable similarities included pronounced pronation of the first metatarsal head, intrinsic rotation of the first metatarsal bone, and rotation of the first tarsal–metatarsal joint, in conjunction with a more supinated naviculocuneiform joint. Our study revealed that both intrinsic pronation of the first metatarsal and pronation at the first tarsal–metatarsal joint were associated with the presence of HV deformity and that naviculocuneiform joint supination was moderately correlated with both the HV and IM angles, suggesting that midfoot rotation may also be relevant to HV morphology.

In terms of correlation, the axial talar–first metatarsal angle was identified as the only axial plane parameter correlated with the absolute HV angle and IM angle, whereas the axial talonavicular angle showed no correlation with HV. These results imply that the inward orientation of the first metatarsal relative to the navicular might be associated with HV deformity. Although the identification of this parameter may be attributed to the commonly observed larger IM angle in patients with HV, the inward alignment of the first metatarsal in relation to the hindfoot could enhance lateral forces on the hallux, potentially relating to the severity of HV.

Increased pronation of the metatarsal head is widely observed in patients with HV. Prior reports indicated that the average α angle in patients with HV ranged from 13.7 to 21.9 degrees, compared with 5.7 to 13.8 degrees in control groups,[22,26] and that the hindfoot moment arm showed an increased correlation with the α angle under conditions of an abnormal Meary angle.[38] In our study, we extended our analysis to include patients with PCFD. In our patient cohort, the average Meary angle was −27.8 degrees, and the

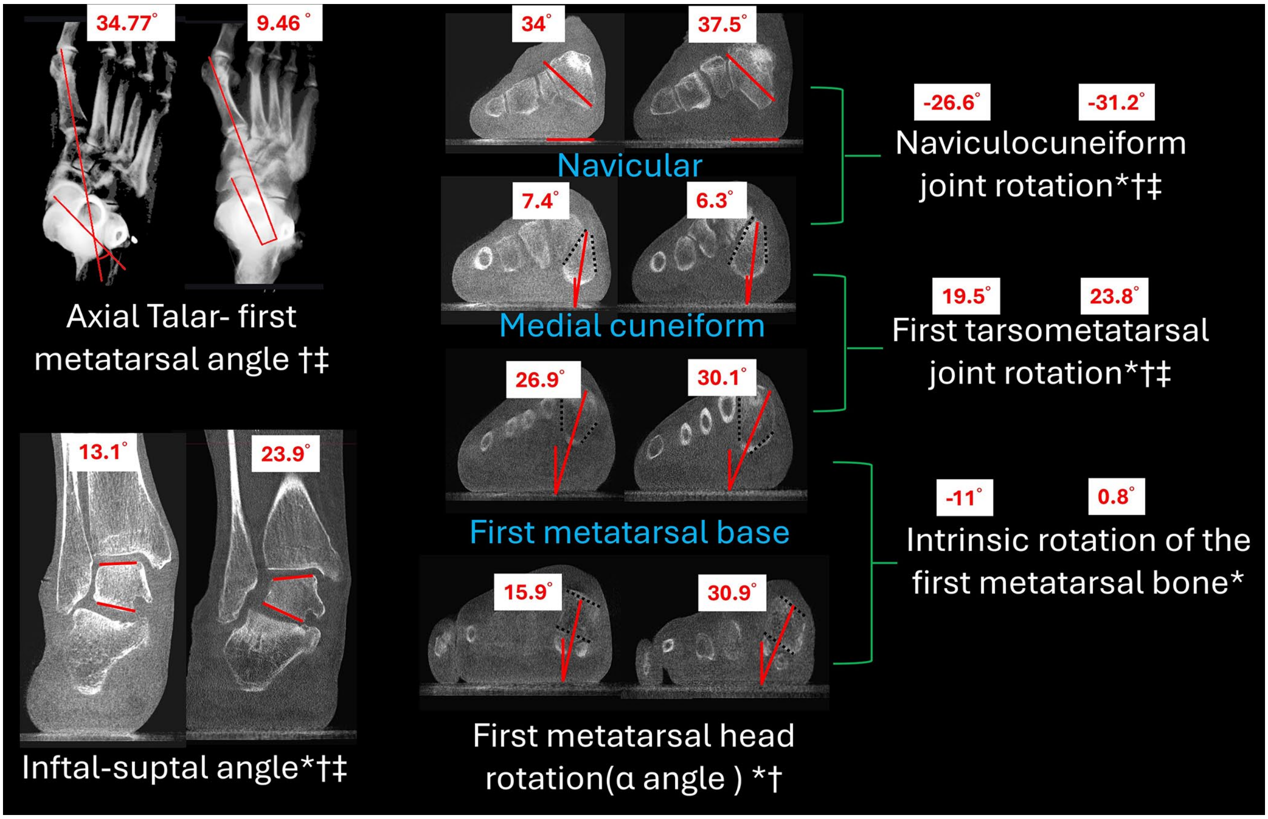

Figure 3. Depiction of radiographic parameters (displayed in white font) incorporated into the generalized estimating equation (GEE) regression analysis for the presence of hallux valgus (HV) deformity (defined as an HV angle of ≥15 degrees). In the comparative illustrations, the image on the left is of a 71-year-old male patient with an HV angle of 12.83 degrees, categorized under the progressive collapsing foot deformity (PCFD) without HV group. In contrast, the image on the right is of a 76-year-old female patient with an HV angle of 24.32 degrees, categorized under the PCFD with HV group. Black dashed lines represent tangent lines of the bone surface. Red lines signify the measurement of each parameter, whereas the green lines illustrate the discrepancy between the 2 sets of measured values. Red numbers denote the values of the measurements. [See online article for color figure.]
*GEE parameter selection *P* value < .1. †Significant correlation with the HV angle. ‡Significant correlation with the intermetatarsal angle.

average hindfoot moment arm was 13.2 mm, with an observed average metatarsal head pronation of 20.7 degrees. These results seem to corroborate the concurrent pronation of the first metatarsal head and hindfoot noted in previous studies.[4,38] However, despite the close association between the pronation of the first metatarsal head and sesamoid position,[12] which could theoretically affect the balance of the metatarsophalangeal joint, only 33 (45.8%) of 72 feet analyzed in our study had HV deformity. In fact, our findings indicate that rotation of the first metatarsal head is only weakly correlated with the HV angle ($\rho=0.312$, $P=.008$), and there is no correlation with the IM angle ($\rho=0.203$, $P=.152$) in patients with PCFD. Additionally, first metatarsal head rotation was not significantly associated with the presence of HV deformity in our regression model ($P=.420$). Moreover, none of the parameters indicating the severity of hindfoot valgus in our study, including hindfoot moment arm, hindfoot angle, and foot and ankle offset, were correlated with HV severity. Further, none of these parameters were significantly associated with HV deformity. Instead, the infratalar-supratalar angle, previously identified as being strongly associated with the presence of symptomatic PCFD,[2,10] was the only hindfoot parameter that correlated with HV deformity. Theoretically, a more valgus infratalar-supratalar angle indicates a more vertical orientation of the subtalar joint. In the context of similar hindfoot alignment, reduced skeletal support may lead to increased strain on the medial soft tissues, including the abductor hallucis muscle, during weightbearing activities. However, dynamic experiments or longitudinal studies are needed to confirm this theory.

This study has some limitations. First, as a radiographic study, measurement bias might have affected the outcomes. Nonetheless, we expended efforts to mitigate this by establishing a clear measurement protocol and adopting semiautomated and manually measured parameters with proven accuracy to minimize potential errors.[13,16,24,34] Second, WBCT was used as the primary tool for examining

Table 4. Generalized Estimating Equation Regression Model Parameter Selection and Results.

Parameters	Selection Reason	Effect Size	Estimate	Robust SE	*P* Value
Intercept			−6.682	2.211	.003
Female sex	Effect size > 0.8	.892	−0.325	0.871	.709
Axial talar–first metatarsal angle	Significantly correlated with HVA and IMA	.531			
Infratalar-supratalar angle	1. GEE parameter selection *P* value[a] < .1 2. Significantly correlated with HVA and IMA	.608	0.217	0.074	.004[b]
Naviculocuneiform joint	1. GEE parameter selection *P* value[a] < .1 2. Significantly correlated with HVA and IMA	.479			
First tarsal–metatarsal joint	1. GEE parameter selection *P* value[a] < .1 2. Significantly correlated with HVA and IMA	.604	0.328	0.076	< .001[b]
	GEE parameter selection *P* value[a] < .1	.616	0.456	0.115	< .001[b]
First metatarsal head (α angle)	1. GEE parameter selection *P* value[a] < .1 2. Significantly correlated with HVA	.649	−0.065	0.080	.420

Abbreviations: GEE, generalized estimating equation; SE, standard error; ρ, Spearman correlation coefficient; HVA, hallux valgus angle; IMA, intermetatarsal angle.
[a]Adjusted using the Benjamini-Hochberg method.
[b]$P < .05$.

anatomical differences between the PCFD with HV group and the PCFD without HV group. However, the severity of soft tissue degeneration in patients with PCFD may also be a major cause of HV deformities. Additional soft tissue studies, including magnetic resonance imaging, should be integrated into future investigations. Third, because of the small case number and inclusion of both feet in some patients (14 of 58), potential errors may have arisen. We aimed to minimize the impact of these factors by using the GEE statistical method and calculating effect sizes. Fourth, although structural and alignment differences between the PCFD with HV group and PCFD without HV group were identified, causal relationships between these differences and HV development in patients could not be definitively established in our study because of its retrospective nature. Further longitudinal studies are required to augment our understanding of the relationship between PCFD and HV. Finally, this study was static, and the posture of patients undergoing WBCT as well as foot weightbearing distribution could have influenced the results. Dynamic examinations, such as gait analysis, may serve as future research directions.

Conclusions

Our results showed that there are indeed anatomical differences between patients with PCFD and HV and patients with PCFD without HV. Among these differences, valgus of the infratalar-supratalar angle is the only hindfoot parameter significantly associated with the presence of HV. Regarding medial column rotational profiles, pronation at the first tarsometatarsal joint, and intrinsic pronation of the first metatarsal bone were significantly associated with HV deformity. Besides these parameters, the axial talar–first metatarsal angle showed a significant correlation with the absolute values of the HV angle and IM angle. By identifying these differences, we hope this study can serve as a foundation for future prospective longitudinal studies or dynamic research to further explore the relationships between PCFD and HV.

Ethical Approval

Ethical approval for this study was obtained from Duke University health System Institutional Review Board (IRB Pro00113556).

Declaration of Conflicting Interests

The author(s) declared the following potential conflicts of interest with respect to the research, authorship, and/or publication of this article: Cesar de Cesar Netto, MD, PhD, reports financial interests in CurveBeam, Paragon 28, and Disior, companies whose software has been specifically used for measuring radiographic parameters in this research. These interests include equity, royalties, advisory roles, and paid consultancy, and are compliant with applicable regulations and Duke University's policies. Disclosure forms for all authors are available online.

Funding

The author(s) received no financial support for the research, authorship, and/or publication of this article.

ORCID iDs

Chien-Shun Wang, MD, https://orcid.org/0000-0001-8707-1108
Grayson M. Talaski, https://orcid.org/0000-0002-0018-6410
Antoine S. Acker, MD, https://orcid.org/0000-0002-4103-6136
Cesar de Cesar Netto, MD, PhD, https://orcid.org/0000-0001-6037-0685

References

1. Albano D, Martinelli N, Bianchi A, et al. Posterior tibial tendon dysfunction: clinical and magnetic resonance imaging

findings having histology as reference standard. *Eur J Radiol*. 2018;99:55-61. doi:10.1016/j.ejrad.2017.12.005

2. Apostle KL, Coleman NW, Sangeorzan BJ. Subtalar joint axis in patients with symptomatic peritalar subluxation compared to normal controls. *Foot Ankle Int*. 2014;35(11):1153-1158. doi:10.1177/1071100714546549
3. Atbasi Z, Erdem Y, Kose O, Demiralp B, Ilkbahar S, Tekin HO. Relationship between hallux valgus and pes planus: Real or fiction? *J Foot Ankle Surg*. 2020;59(3):513-517. doi:10.1053/j.jfas.2019.09.037
4. Bakshi N, Steadman J, Philippi M, et al. Association between hindfoot alignment and first metatarsal rotation. *Foot Ankle Int*. 2022;43(1):105-112. doi:10.1177/107110072 11033514
5. Barg A, Harmer JR, Presson AP, Zhang C, Lackey M, Saltzman CL. Unfavorable outcomes following surgical treatment of hallux valgus deformity: a systematic literature review. *J Bone Joint Surg Am*. 2018;100(18):1563-1573. doi:10.2106/JBJS.17.00975
6. Cacace L, Hillstrom H, Dufour A, Hannan M. The association between pes planus foot type and the prevalence of foot disorders: the Framingham Foot Study. *Osteoarthritis Cartilage*. 2013;21:S166-S167.
7. Campbell B, Miller MC, Williams L, Conti SF. Pilot study of a 3-dimensional method for analysis of pronation of the first metatarsal of hallux valgus patients. *Foot Ankle Int*. 2018;39(12):1449-1456. doi:10.1177/1071100718793391
8. Cheney N, Rockwell K, Long J, et al. Is a flatfoot associated with a hallux valgus deformity? *Foot Ankle Orthop*. 2017;2(3): 2473011417S2473000133.
9. Chinn S. A simple method for converting an odds ratio to effect size for use in meta-analysis. *Stat Med*. 2000;19(22):3127-3131. doi:10.1002/1097-0258(20001130)19:22<3127::aid-sim784>3.0.co;2-m
10. Cody EA, Williamson ER, Burket JC, Deland JT, Ellis SJ. Correlation of talar anatomy and subtalar joint alignment on weightbearing computed tomography with radiographic flatfoot parameters. *Foot Ankle Int*. 2016;37(8):874-881. doi:10.1177/1071100716646629
11. Conti MS, MacMahon A, Ellis SJ, Cody EA. Effect of the modified Lapidus procedure for hallux valgus on foot width. *Foot Ankle Int*. 2020;41(2):154-159. doi:10.1177/1071100719884556
12. Dayton P, Kauwe M, DiDomenico L, Feilmeier M, Reimer R. Quantitative analysis of the degree of frontal rotation required to anatomically align the first metatarsal phalangeal joint during modified tarsal-metatarsal arthrodesis without capsular balancing. *J Foot Ankle Surg*. 2016;55(2):220-225. doi:10.1053/j.jfas.2015.08.018
13. de Cesar Netto C, Bang K, Mansur NS, et al. Multiplanar semiautomatic assessment of foot and ankle offset in adult acquired flatfoot deformity. *Foot Ankle Int*. 2020;41(7):839-848. doi:10.1177/1071100720920274
14. de Cesar Netto C, Shakoor D, Dein EJ, et al. Influence of investigator experience on reliability of adult acquired flatfoot deformity measurements using weightbearing computed tomography. *Foot Ankle Surg*. 2019;25(4):495-502. doi:10.1016/j.fas.2018.03.001
15. Deland JT. Adult-acquired flatfoot deformity. *J Am Acad Orthop Surg*. 2008;16(7):399-406. doi:10.5435/00124635-200807000-00005
16. Dibbern K, Briggs H, Behrens A, et al. Reliability of coronal plane rotation measurements in the medial column of the foot: a cadaveric study. *J Foot Ankle*. 2021;15(3):252-258.
17. Fayed A, Mallavarapu V, Schmidt E, et al. Deformities influencing different classes in progressive collapsing foot. *Iowa Orthop J*. 2023;43(2):8-13.
18. Ferri M, Scharfenberger AV, Goplen G, Daniels TR, Pearce D. Weightbearing CT scan of severe flexible pes planus deformities. *Foot Ankle Int*. 2008;29(2):199-204. doi:10.3113/FAI.2008.0199
19. Funk DA, Cass JR, Johnson KA. Acquired adult flat foot secondary to posterior tibial-tendon pathology. *J Bone Joint Surg Am*. 1986;68(1):95-102.
20. Hardy RH, Clapham JC. Observations on hallux valgus; based on a controlled series. *J Bone Joint Surg Br*. 1951;33-B(3):376-391. doi:10.1302/0301-620X.33B3.376
21. Heyes GJ, Vosoughi AR, Weigelt L, Mason L, Molloy A. Pes planus deformity and its association with hallux valgus recurrence following scarf osteotomy. *Foot Ankle Int*. 2020;41(10):1212-1218. doi:10.1177/1071100720937645
22. Kim Y, Kim JS, Young KW, Naraghi R, Cho HK, Lee SY. A new measure of tibial sesamoid position in hallux valgus in relation to the coronal rotation of the first metatarsal in CT scans. *Foot Ankle Int*. 2015;36(8):944-952. doi:10.1177/1071100715576994
23. Krahenbuhl N, Kvarda P, Susdorf R, et al. Assessment of progressive collapsing foot deformity using semiautomated 3D measurements derived from weightbearing CT scans. *Foot Ankle Int*. 2022;43(3):363-370. doi:10.1177/10711007211049754
24. Kvarda P, Krahenbuhl N, Susdorf R, et al. High reliability for semiautomated 3D measurements based on weightbearing CT scans. *Foot Ankle Int*. 2022;43(1):91-95. doi:10.1177/10711007211034522
25. Lalevee M, Barbachan Mansur NS, Dibbern K, et al. Coronal plane rotation of the medial column in hallux valgus: a retrospective case-control study. *Foot Ankle Int*. 2022;43(8):1041-1048. doi:10.1177/10711007221091810
26. Lalevee M, Barbachan Mansur NS, Lee HY, et al. Distal metatarsal articular angle in hallux valgus deformity. Fact or fiction? A 3-dimensional weightbearing CT assessment. *Foot Ankle Int*. 2022;43(4):495-503. doi:10.1177/10711007211051642
27. Lalevee M, Barbachan Mansur NS, Schmidt E, et al. Does tibialis posterior dysfunction correlate with a worse radiographic overall alignment in progressive collapsing foot deformity? A retrospective study. *Foot Ankle Surg*. 2022;28(7):995-1001. doi:10.1016/j.fas.2022.02.004
28. Langan TM, Greschner JM, Brandao RA, Goss DA Jr, Smith CN, Hyer CF. Maintenance of correction of the modified Lapidus procedure with a first metatarsal to intermediate cuneiform cross-screw technique. *Foot Ankle Int*. 2020;41(4):428-436. doi:10.1177/1071100719895268
29. Lintz F, Jepsen M, De Cesar Netto C, et al. Distance mapping of the foot and ankle joints using weightbearing CT: the

cavovarus configuration. *Foot Ankle Surg*. 2021;27(4):412-420. doi:10.1016/j.fas.2020.05.007
30. Lintz F, Welck M, Bernasconi A, et al. 3D biometrics for hindfoot alignment using weightbearing CT. *Foot Ankle Int*. 2017;38(6):684-689. doi:10.1177/1071100717690806
31. Mahmoud K, Metikala S, Mehta SD, Fryhofer GW, Farber DC, Prat D. The role of weightbearing computed tomography scan in hallux valgus. *Foot Ankle Int*. 2021;42(3):287-293. doi:10.1177/1071100720962398
32. Najefi AA, Malhotra K, Patel S, Cullen N, Welck M. Assessing the rotation of the first metatarsal on computed tomography scans: a systematic literature review. *Foot Ankle Int*. 2022;43(1):66-76. doi:10.1177/10711007211020676
33. Nguyen US, Hillstrom HJ, Li W, et al. Factors associated with hallux valgus in a population-based study of older women and men: the mobilize Boston study. *Osteoarthritis Cartilage*. 2010;18(1):41-46. doi:10.1016/j.joca.2009.07.008
34. Probasco W, Haleem AM, Yu J, Sangeorzan BJ, Deland JT, Ellis SJ. Assessment of coronal plane subtalar joint alignment in peritalar subluxation via weight-bearing multiplanar imaging. *Foot Ankle Int*. 2015;36(3):302-309. doi:10.1177/1071100714557861
35. Saltzman CL, Brandser EA, Anderson CM, Berbaum KS, Brown TD. Coronal plane rotation of the first metatarsal. *Foot Ankle Int*. 1996;17(3):157-161. doi:10.1177/107110079601700307
36. Saltzman CL, el-Khoury GY. The hindfoot alignment view. *Foot Ankle Int*. 1995;16(9):572-576. doi:10.1177/107110079501600911
37. Saltzman CL, Nawoczenski DA, Talbot KD. Measurement of the medial longitudinal arch. *Arch Phys Med Rehabil*. 1995;76(1):45-49. doi:10.1016/s0003-9993(95)80041-7
38. Steadman J, Bakshi N, Philippi M, et al. Association of normal vs abnormal Meary angle with hindfoot malalignment and first metatarsal rotation: a short report. *Foot Ankle Int*. 2022;43(5):706-709. doi:10.1177/10711007211068473
39. Steadman J, Barg A, Saltzman CL. First metatarsal rotation in hallux valgus deformity. *Foot Ankle Int*. 2021;42(4):510-522. doi:10.1177/1071100721997149
40. Suh DH, Kim HJ, Park JH, Park YH, Koo BM, Choi GW. Relationship between hallux valgus and pes planus in adult patients. *J Foot Ankle Surg*. 2021;60(2):297-301. doi:10.1053/j.jfas.2020.06.030
41. Talbot KD, Saltzman CL. Hallucal rotation: a method of measurement and relationship to bunion deformity. *Foot Ankle Int*. 1997;18(9):550-556. doi:10.1177/107110079701800904
42. Zaidi R, Sangoi D, Cullen N, Patel S, Welck M, Malhotra K. Semi-automated 3-dimensional analysis of the normal foot and ankle using weight bearing CT - a report of normal values and bony relationships. *Foot Ankle Surg*. 2023;29(2):111-117. doi:10.1016/j.fas.2022.12.001